Acta Biomaterialia xxx (2014) xxx–xxx

Contents lists available at ScienceDirect

Acta Biomaterialia

journal homepage: www.elsevier.com/locate/actabiomat

Surface-templated hydrogel patterns prompt matrix-dependent migration of breast cancer cells towards chemokine-secreting cells

Taisuke Kojima [a,c], Christopher Moraes [b,c], Stephen P. Cavnar [b,c], Gary D. Luker [b,d,e,*], Shuichi Takayama [a,b,c,*]

[a] Macromolecular Science and Engineering Program, University of Michigan, Ann Arbor, MI, USA
[b] Department of Biomedical Engineering, University of Michigan, Ann Arbor, MI, USA
[c] Biointerfaces Institute, University of Michigan, Ann Arbor, MI, USA
[d] Center for Molecular Imaging, Department of Radiology, University of Michigan, Ann Arbor, MI, USA
[e] Department of Microbiology and Immunology, University of Michigan, Ann Arbor, MI, USA

ARTICLE INFO

Article history:
Received 23 June 2014
Received in revised form 5 November 2014
Accepted 14 November 2014
Available online xxxx

Keywords:
Hydrogels
Cell migration
Surface modification
Micropatterning, Gradient

ABSTRACT

This paper describes a novel technique for fabricating spatially defined cell-laden collagen hydrogels, using patterned, non-adhesive polyacrylamide-coated polydimethylsiloxane (PDMS) surfaces as a template. Precisely patterned embedded co-cultures of breast cancer cells and chemokine-producing cells generated with this technique revealed matrix-dependent and chemokine isoform-dependent migration of cancer cells. CXCL12 chemokine-secreting cells induce significantly more chemotaxis of cancer cells when the 3-D extracellular matrix (ECM) includes components that bind the secreted CXCL12 chemokines. Experimental observations using cells that secrete CXCL12 isoforms with different matrix affinities together with computational simulations show that stronger ligand–matrix interactions sharpen chemoattractant gradients, leading to increased chemotaxis of the CXCL12 gradient-sensing CXCR4 receptor-expressing (CXCR4+) cells patterned in the hydrogel. These results extend our recent report on CXCL12 isoform-dependent chemotaxis studies from 2-D to 3-D environments and additionally reveal the important role of ECM composition. The developed technology is simple, versatile and robust; and as chemoattractant-matrix interactions are common, the methods described here should be broadly applicable for study of physiological migration of many different cell types in response to a variety of chemoattractants.

1. Introduction

Gradient formation and sensing is a complicated process involved in many physiological and pathological processes. Cells will change morphology and move toward a chemical gradient depending on the shape, dynamics and magnitude of the gradient [1]. The simplest model of gradient formation involves diffusion of soluble factors away from cells that secrete them. However, in vivo there are two types of microenvironmental interactions that define gradient formation and sensing: ligand–matrix and ligand–cell. Several studies have demonstrated the importance of complex gradient shape and dynamics in vivo, driven by ligand–matrix interactions [2,3] and by active cell-dependent ligand scavenging [4]. Hence, to properly model and experimentally manipulate these complex chemotactic processes, we need experimental systems that recreate these environmental influences on gradient formation. In this work, we develop a technique that enables robust and versatile definition of in vitro multicellular/microenvironment interactions, in physiologically relevant 3-D environments, and utilize this technique to study the relationship between ligand–matrix and ligand–cell interactions on migration of breast cancer cells.

A few in vitro assays exist to recreate how ligand–matrix and ligand–cell interactions collectively guide gradient formation. Transwells [5], hydrogels [6–10] and microchannels [11–16] are typically used to spatially pattern cells, define morphogenetic and chemotactic gradients, and monitor cell morphology and chemotaxis. Although these assays isolate individual aspects of gradient formation and sensing, they fail to replicate how multiple cell types and matrix interactions together define a gradient. We previously developed an experimental source-sink system to replicate the formation of defined soluble gradients between spatially

* Corresponding authors at: A728 Biomedical Sciences Research Building, 109 Zina Pitcher Place, Ann Arbor, MI 48109, USA. Tel.: +1 (734) 763 5476; fax: +1 (734) 763 5447 (G.D. Luker). A183 Building 10 NCRC, 2800 Plymouth Road, Ann Arbor, MI 48109, USA. Tel.: +1 (734) 615 5539; fax: +1 (734) 936 1905 (S. Takayama).
E-mail addresses: gluker@med.umich.edu (G.D. Luker), takayama@umich.edu (S. Takayama).

http://dx.doi.org/10.1016/j.actbio.2014.11.033
1742-7061/

patterned cells that secrete ligands (source) and cells that scavenge ligands (sink) [17,18]. These previous studies capture the involvement of multiple cell types in source-sink gradient formation and the role of ligand binding to the device- and cell-surfaces. However, the relatively small surface area with limited amount of binding sites available in this simple 2-D assay is not sufficient to address the potential influence of ligand–matrix interactions, as compared to the in vivo situation in which 3-D matrices provide a significantly greater concentration of binding sites.

In this work, we develop a novel patterning system to spatially pattern cells within an extracellular matrix (ECM), creating a model tissue-like environment for studies of directional cell migration. There are several techniques to create desired hydrogel patterns, such as laser lithography [19–25] and microchannel guides [26–28], that often require significant expertise, specialized instruments and complicated processing. Our approach enables the precise positioning of multiple cell types within a 3-D matrix, using relatively simple tools and expertise that should be accessible to most wet-labs. As a first application of this technology, we spatially pattern cells engineered to secrete the α- and β-isoforms of the CXCL12 chemokine and CXCR4 + cells that respond to CXCL12, while varying the composition of the surrounding matrix. Using this breast cancer model system, we demonstrate (i) the ability to systematically control ligand–matrix interactions via matrix composition; (ii) the ability to spatially pattern multiple interacting cell types within a 3-D matrix; and (iii) the effects of ligand–matrix interactions on gradient formation, and on subsequent cell migration.

2. Materials and methods

Unless otherwise stated, all chemicals and reagents for cell culture were purchased from Sigma–Aldrich, fluorescent dyes from Invitrogen, and all other equipment and materials from Fisher Scientific.

2.1. Cell culture

MDA-MB-231 (231, ATCC) cells were primarily used for these experiments, and were cultured in fully supplemented Dulbecco's modified Eagle's medium (DMEM, with 10% fetal bovine serum (FBS), 1% antibiotics–antimycotics). Some demonstration experiments were conducted with NIH 3T3 murine fibroblasts (cultured in fully supplemented DMEM) and human bone marrow endothelial cells (HBMECs, a gift from Irma de Jong, cultured in fully supplemented endothelial cell growth media (EGM2) with 5% FBS; Lonza). Standard trypsinization-based subculture protocols were used to passage cells prior to the experiment. We previously described culture, lentiviral transduction and migration of 231 cells expressing CXCR4 towards 231 cells secreting CXCL12 [17,18]. Briefly, we transduced 231 cells sequentially with a CXCR4-GFP fusion [29] and NLS-AcGFP to facilitate receptor-based migration and image-based tracking of nuclei [18], respectively. We expressed CXCL12-isoforms fused to *Gaussia* luciferase (GL) upstream of the fluorescent protein mCherry in a pLVX IRES vector, to facilitate proportional fluorescence sorting for CXCL12-expressing cells [18].

2.2. Preparation of PAA-coated PDMS surface

A 10:1 (w/w) degassed mixture of polydimethylsiloxane (PDMS) and a curing agent was diluted with toluene (PDMS:toluene = 1:3). 12 mm diameter glass slides were dipped into the mixed solution and baked at 120 °C for 30 min. A 9:1 (v/v) mixture of prepolymer solution (18.9 wt.% acrylamide, 0.33 wt.% pluronic F108 and 80.77 wt.% water) and photoinitiator solution (0.3 wt.% benzophenone and 99.7 wt.% 2-propanol) were added to the PDMS-coated slides and polymerized under UV (CL-1000, UVP: 8 W × 4 min) followed by an extensive wash in water [30,31]. The polyacrylamide (PAA)-coated PDMS slides were stored at ambient conditions and used for following hydrogel patterning within a few days (Fig. 1A).

2.3. Fabrication of oxidized patterns

The SU-8 master molds were fabricated by soft lithography. The detailed procedure for fabrication of master molds can be found elsewhere [32]. The PDMS replicas of patterns which served as oxidation stencils were placed in conformal contact with the PAA-coated PDMS slides and oxidized (100 W × 10 min) [33]. Oxidized PAA-coated PDMS slides were immediately used for hydrogel patterning (Fig. 1B).

2.4. Surface characterization

Water contact angles in air were measured on PDMS-coated slides and PAA-coated PDMS slides before and after oxidation by the sessile drop technique (4 μl of water) using a goniometer and analyzed with ImageJ. Data are expressed as a mean ± standard deviation (n = 3). Surface topography of PAA-coated PDMS slides oxidized through patterns was measured using a Bruker Veeco atomic force microscope in ScanAsyst mode, and analyzed with a Nanoscope (Veeco, Bruker).

2.5. Hydrogel patterning

2 ml of degassed PDMS was poured and cured into each well of a 6-well plate (Fig. 1C). Each PDMS well was punched along the shape of a 12 mm glass slide and each oxidized PAA-coated PDMS slide was set at the bottom of the well. Trypsinized cells were mixed with neutralized type I bovine collagen (BD Biosciences) to create a suspension of 10 million cells ml^{-1} in 2 mg ml^{-1} of collagen. For cell-free experiments, 1 μm diameter fluorescent beads (Sigma) were added to the neutralized collagen solution. 6 μl of the collagen gel solution was dispensed over each adhesive pattern and allowed to polymerize for 45 min in a humidified cell incubator (37 °C, 5% CO2). 250 μl of either 2.5 mg ml^{-1} neutralized collagen or 2.5 mg ml^{-1} neutralized collagen supplemented with a growth factor reduced Matrigel (BD Biosciences: 61% laminin, 30% collagen IV, 7% entacin and 2% other proteins including proteoglycans) mixture of collagen gel and matrigel solutions (75 vol.% collagen I + 25 vol.% Matrigel) was poured on each well and allowed to polymerize for 1 h in the humidified incubator. 2 ml of cell culture media were added to each well and cultured at 37 °C. For observation of non-specific cellular movement, Latrunculin (10 μM) was added to the media in control samples to prevent actin polymerization and hence migration.

2.6. Cell adhesion test

DMEM cell culture media containing MDA-MB-231 cells was cultured on tissue culture plastic, PAA-coated PDMS or oxidized PAA-coated PDMS slides in a 24-well plate and incubated for 24 h. Cell culture media was aspirated and samples were rinsed twice in PBS. 1 ml of 4% paraformaldehyde solution was added to fix cells. Cellular actin cytoskeletal structures and the cell nucleus were labeled with Phalloidin and Hoechst dyes, following protocols obtained from the manufacturers. Images were collected with an epifluorescent microscope (TE-300, Nikon) and analyzed with ImageJ to determine cell density and spread area, expressed as a mean ± standard deviation (n = 6).

Please cite this article in press as: Kojima T et al. Surface-templated hydrogel patterns prompt matrix-dependent migration of breast cancer cells towards chemokine-secreting cells. Acta Biomater (2014), http://dx.doi.org/10.1016/j.actbio.2014.11.033

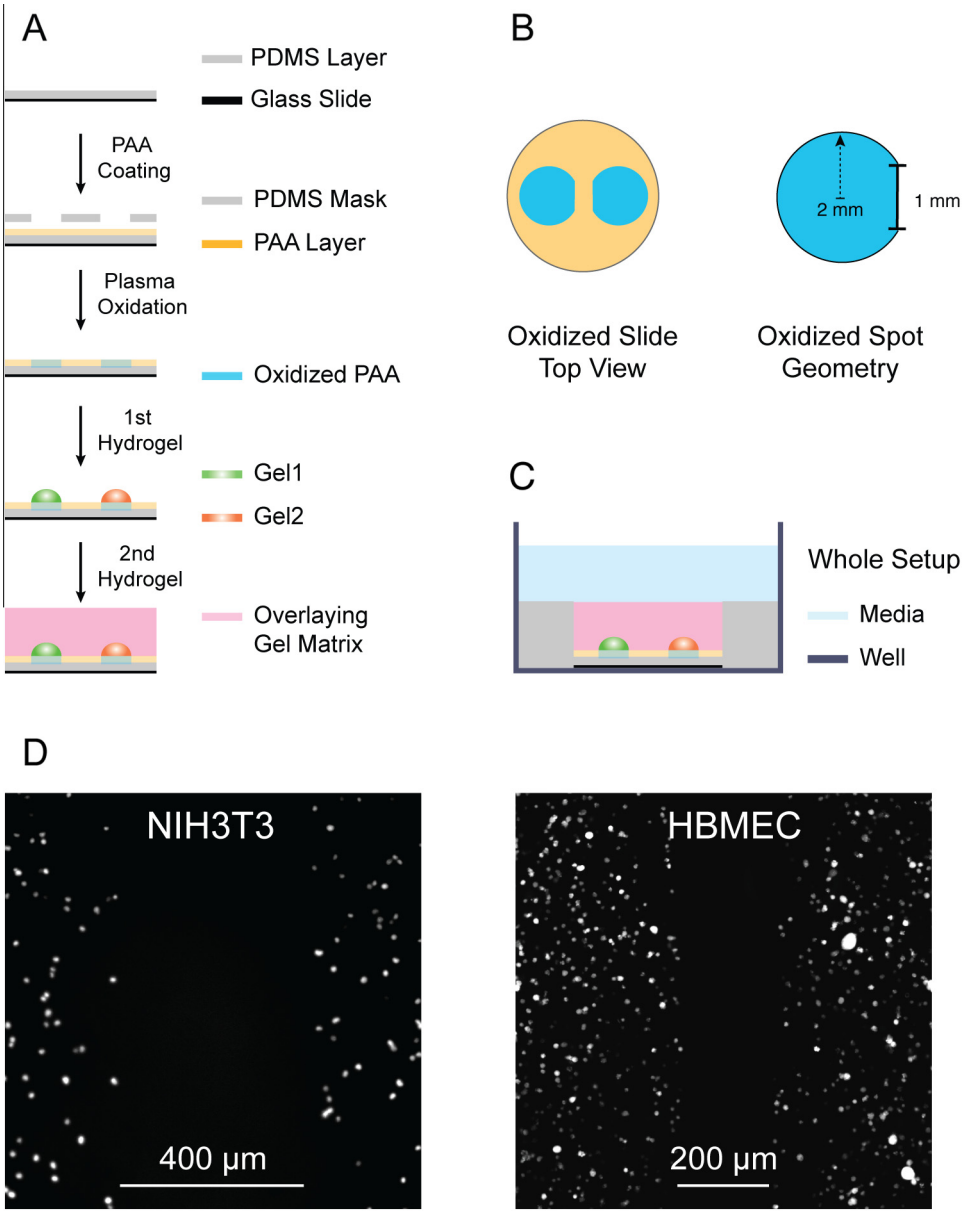

Fig. 1. Patterning of hydrogels on a cell-repellent surface. (A) PAA was polymerized on PDMS-coated glass slides and oxidized along mask patterns. Hydrogel precursor solutions are added to oxidized regions and cured. Gel solution was overlaid on the patterns and incubated for measurement. (B) Top view illustration of a patterned slide. Whole slide 12 mm diameter and oxidized spot 4 mm diameter. (C) Side view illustration of the whole setup. (D) Fluorescent image of patterned collagen gels containing NIH3T3 cells overlaid by collagen gel with 400 µm pattern-to-pattern distance and fluorescent image of patterned collagen gels containing HBMECs overlaid by the mixed gel (60 vol.% Matrigel + 40 vol.% collagen gel) with 200 µm pattern-to-pattern distance. Scale bar 400 um for NIH3T3 and 200 µm for HBMEC.

2.7. Modeling diffusion and binding kinetics

Finite-element modelling of the diffusion and binding kinetics was conducted in COMSOL 4.2 (Burlington, MA), using a 1-D model geometry. Parameters for diffusion of CXCL12 (MW ≈ 10 kDa) were estimated based on the Stokes–Einstein equation relating hydrodynamic radius to diffusion rate, and published values in the literature for diffusion of large molecules in collagen [34]. The flux of CXCL12 molecules at one end of the model was calculated based on the estimated rate of CXCL12 production by cells [18] and on the geometry of the hydrogel system. A reaction–diffusion COMSOL module was used to simulate binding of the secreted soluble factors to uniformly distributed binding sites, representing Matrigel proteoglycans in the collagen matrix. The kinetic binding parameters of CXCL12-α and CXCL12-β to matrigel proteoglycans were estimated as being similar to the binding kinetics of CXCL12 isoforms to heparan sulfate [35]. Results are reported as concentrations of soluble factors and as specific gradients across the length-scale of an individual cell. The specific gradient was determined by dividing the concentration difference across 50 µm by the average concentration over that distance [17].

2.8. Binding assay of CXCL12 to different matrix coatings

We previously described and characterized the production and activity of CXCL12-isoforms fused to *Gaussia* luciferase [18]. Measurement of *Gaussia* luciferase activity allows quantitative measurements of CXCL12 associated with cells, bound to ECM, and in cell culture supernatants. We collected supernatants from 10^6 cells expressing secreted GL, CXCL12-α-GL, CXCL12-β-GL or GL-negative that were plated in 60 mm dishes. After cells had been adhered in 10% FBS DMEM media overnight, they were washed once in PBS,

Please cite this article in press as: Kojima T et al. Surface-templated hydrogel patterns prompt matrix-dependent migration of breast cancer cells towards chemokine-secreting cells. Acta Biomater (2014), http://dx.doi.org/10.1016/j.actbio.2014.11.033

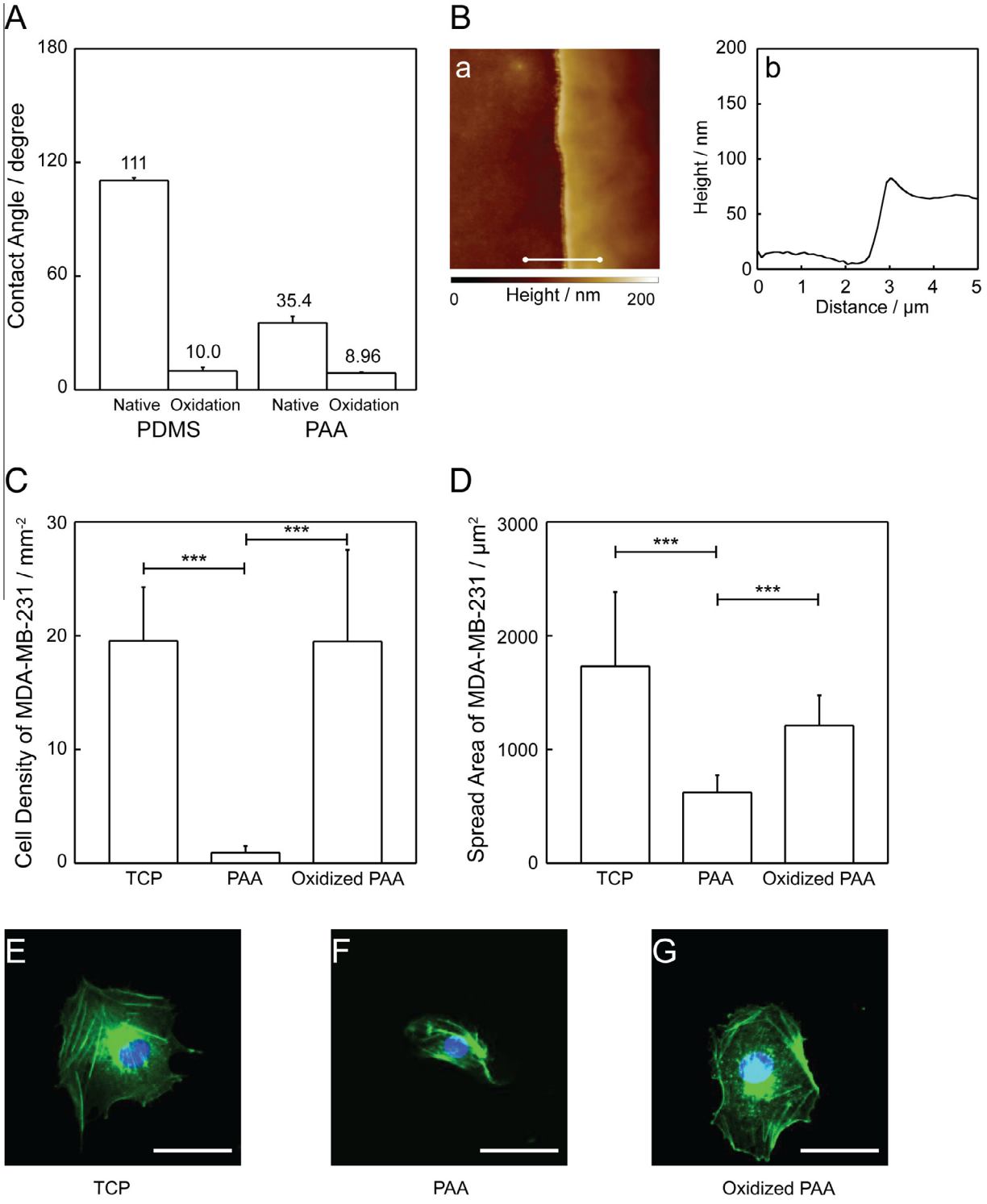

Fig. 2. Surface characterization of PAA-coated PDMS. (A) Contact angle values of water droplet on PDMS, oxidized PDMS, PAA-coated PDMS and oxidized PAA-coated surface. (B) Surface topography of oxidized PAA-coated PDMS. (a) Height profile at the boundary and (b) at the section highlighted by the white bar. (C,D) Cell adhesion test of MDA-MB-231 cells. (C) Cell density and (D) cell spread area of CXCL12-GL on TCP, PAA-coated PDMS and oxidized PAA-coated PDMS. Images of a cell on (E) TCP, (F) PAA-coated PDMS and (G) oxidized PAA-coated PDMS, respectively. Nucleus and cytosol were stained by blue and green, respectively. Scale bar 50 μm.

and media was replenished with DMEM with 0.2% albumin (Probumin Media Grade, Millipore). After 24 h the supernatants were collected and imaged for GL activity and diluted in GL-negative cell supernatants to normalize GL flux activity to that of the lowest condition. Briefly, to measure GL flux, 1 μl of supernatant was assayed in 1:1000 final dilution of the GL-substrate coelanterazine brought to a total volume of 100 μl of PBS, as we have described previously [18]. We added 50 μl of the GL flux-normalized supernatants to 96-well tissue culture plates that were pretreated with ECM (collagen, collagen and Matrigel, Matrigel only, or untreated tissue culture). Pre-treatment was achieved by incubating the 96-well plate with the appropriate solutions at 4 °C for 2 h. The low temperature prevented polymerization but allowed adsorption of both collagen and Matrigel components. Wells were then

Please cite this article in press as: Kojima T et al. Surface-templated hydrogel patterns prompt matrix-dependent migration of breast cancer cells towards chemokine-secreting cells. Acta Biomater (2014), http://dx.doi.org/10.1016/j.actbio.2014.11.033

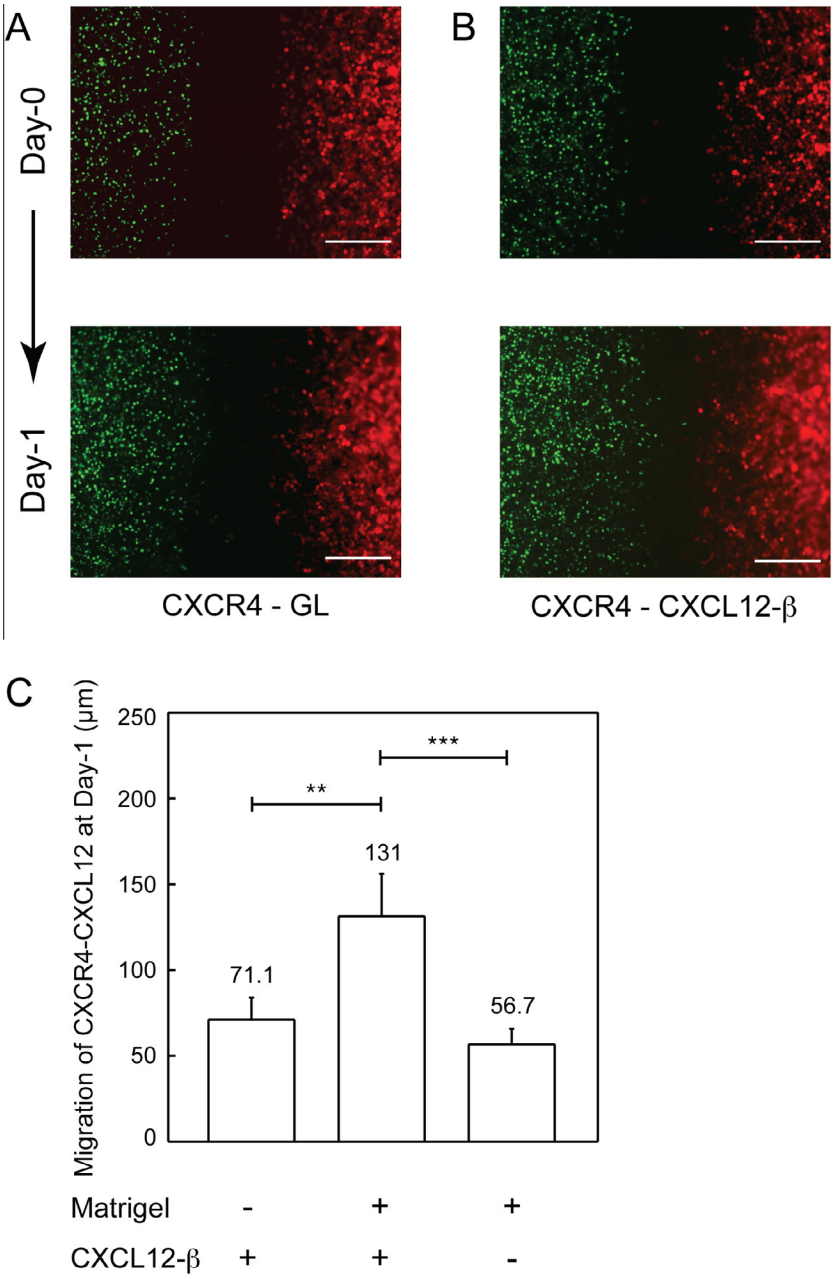

Fig. 3. Migration assay of CXCR4 cells in 3-D gel matrix. (A) Fluorescent images of CXCR4 (green) and GL (red) at day 0 and day 1. (B) Fluorescent images of CXCR4 (green) and CXCL12- β (red) at day 0 and day 1. Scale bar 250 μm. (E) Migration of CXCR4-CXCL12 at day 1 in the absence and presence of Matrigel (**$P < 0.01$; ***$P < 0.001$).

washed twice with PBS. Wells were grouped in quadruplicate for each supernatant type and ECM type for three independent experimental setups. We incubated these plates for 30 min at 37 °C to facilitate binding to the ECM. To remove unbound GL-species, we aspirated medium; washed each well in triplicate with an excess of PBS; and replaced medium with 50 μl of PBS per well. We imaged each well with the same substrate and PBS volumes as above. All bioluminescence images were acquired with the IVIS Lumina Series III (Caliper, LifeSciences), and data were analyzed with Living Image 4.3.1.

2.9. Chemotaxisis of MDA-MB-231 cells

CXCR4 + and source cells (secreted GL as GL, CXCL12-α-GL as CXCL12-α, and CXCL12-β-GL as CXCL12-β) in a mixture of collagen and Matrigel matrix with 2 ml DMEM media were incubated for 24 h and imaged with a fluorescent microscope (TE-300, Nikon). The representative leading cell-to-cell distance at day 0 and day 1 were each measured at five points with ImageJ and expressed as a mean ± standard deviation (n = 6 for GL, n = 6 for CXCL12-α, n = 6 for CXCL12-β, each in the presence of Matrigel, n = 5 for CXCL12-β in the absence of Matrigel).

2.10. Statistical analysis

All statistics are reported as means ± standard deviation. ANOVA tests were performed using a commercially available software package (SigmaStat 3.5; Systat Software Inc., San Jose, CA), using the Tukey test for post hoc pairwise comparisons.

Please cite this article in press as: Kojima T et al. Surface-templated hydrogel patterns prompt matrix-dependent migration of breast cancer cells towards chemokine-secreting cells. Acta Biomater (2014), http://dx.doi.org/10.1016/j.actbio.2014.11.033

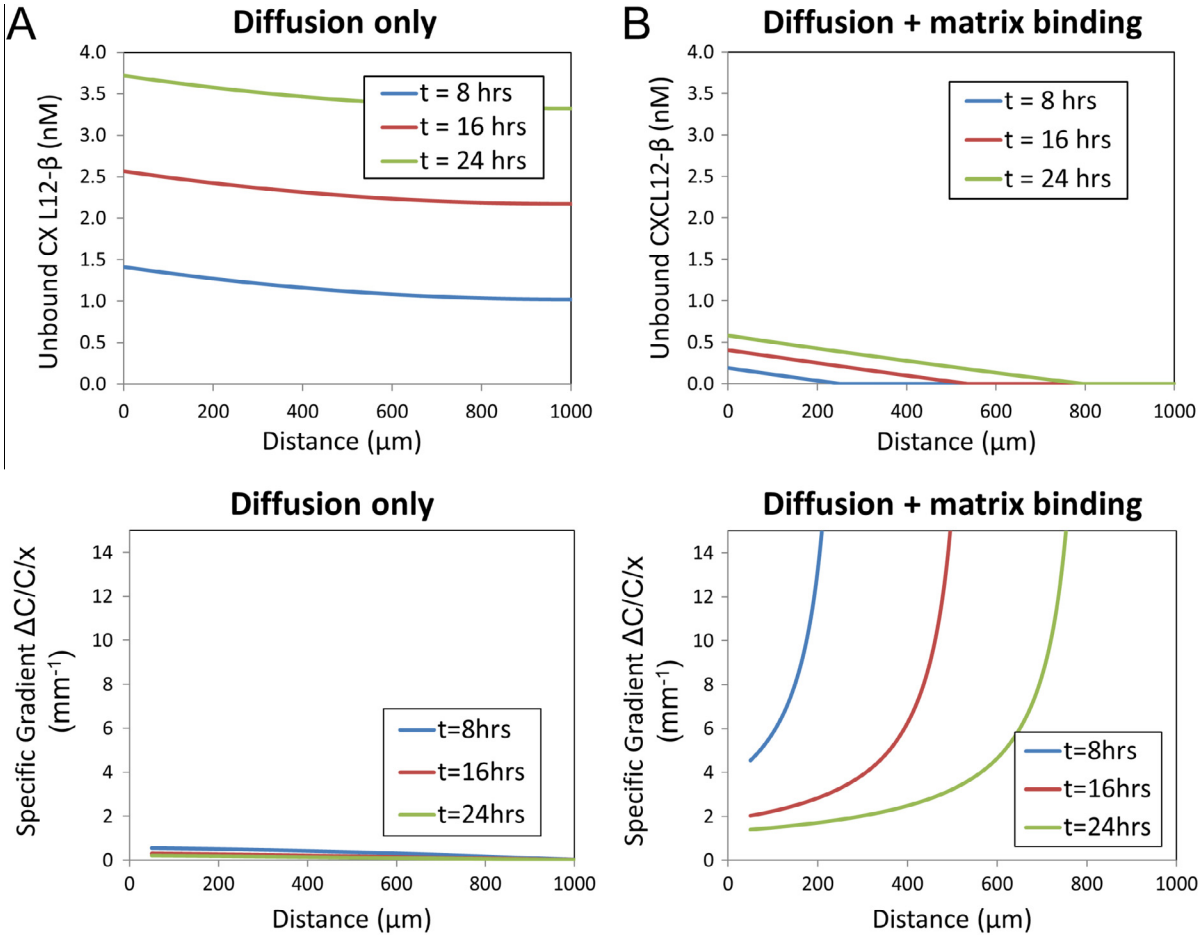

Fig. 4. Computational modeling of CXCL12- β gradients. Simulation of unbound CXCL12- β concentration as a function of distance and time and CXCL12-β-specific gradient (defined as $\Delta C/C_{avg}/x$ across a 50 μm gap) as a function of distance and time when (A) considering only diffusion of unbound signaling molecules, and (B) considering both diffusion and matrix-binding parameters.

3. Results

3.1. Characterization of hydrogel patterns on PAA-coated PDMS

This system enables control of three parameters: spacing between groups of patterned cells, gel composition, and cell type (Fig. 1). PAA-coated PDMS slides were fabricated as described (Fig. 1A–C) and clusters of cells encapsulated in hydrogels were patterned adjacent to each other with defined spacing (Fig. 1D and Fig. S1). The pattern-to-pattern distance was controllable and hydrogel patterns were stable irrespective of cell type and gel composition. Obtaining successful patterns depends on carefully balancing topographic and surface chemistry features of the patterned surface template, at the contact line between the hydrogel precursor solution and the underlying substrate. Surface chemical heterogeneity and physical topology are both known to define the contact line at the liquid–solid and liquid–liquid interface [32,36]. We characterized the surface properties of PAA-coated PDMS by measuring the contact angle of sessile droplets, and by atomic force microscopy (AFM) topographical measurements. The contact angle measurement of native PDMS and PAA-coated PDMS illustrates a dramatic reduction of contact angle before and after plasma oxidation (Fig. 2A). While intact PAA-coated PDMS showed lower contact angle compared to native PDMS due to the hydrophilic nature of PAA introduced on PDMS, both surfaces demonstrated similar contact angles after oxidation. Meanwhile, AFM measurement reveals distinct surface topology of patterned PAA-coated PDMS (Fig. 2B). A clear boundary at the edge of the pattern was observed and the step was ~50 nm at the boundary. In contrast, there was no distinct difference between intact and oxidized PAA-coated PDMS regions (Fig. S2). We confirmed that either reducing oxidation time or leaving substrates for a few days resulted in failure of hydrogel patterning (data not shown), indicating that both surface chemistry and physical topography boundaries are necessary to support the formation of stable hydrogel patterns. We note that the accuracy of the patterning with 250 μm spacing was 246 ± 4.97 μm (n = 3) and the height of a droplet was 0.76 ± 0.041 mm (n = 6). We examined the limitations where the minimum spacing is 100 μm and minimum size of a pattern is 1.5 mm in diameter. Below these dimensions, oxidation and surface treatment did not work properly and failed to sustain the droplet shape.

In addition to the ability to precisely pattern hydrogels, PAA serves as a non-adhesive cell-repellent material [37], and prevents migration of the cells over the PAA surface. To confirm this, the number of cells adhered to these surfaces were assessed using a standard cell-adhesion test, and indicates that adhesion was virtually eliminated, as compared to tissue culture plastic surfaces. Furthermore, cell spread area was also greatly reduced for the few adherent cells (Fig. 2C–G), indicating that cells cannot attach sufficiently to spread, and therefore migrate. Cell adhesion and spreading were restored after oxidation of the PAA surface, but as this occurs only within the regions of patterned cells and not in the region of migration between cell patterns, these effects can be

Please cite this article in press as: Kojima T et al. Surface-templated hydrogel patterns prompt matrix-dependent migration of breast cancer cells towards chemokine-secreting cells. Acta Biomater (2014), http://dx.doi.org/10.1016/j.actbio.2014.11.033

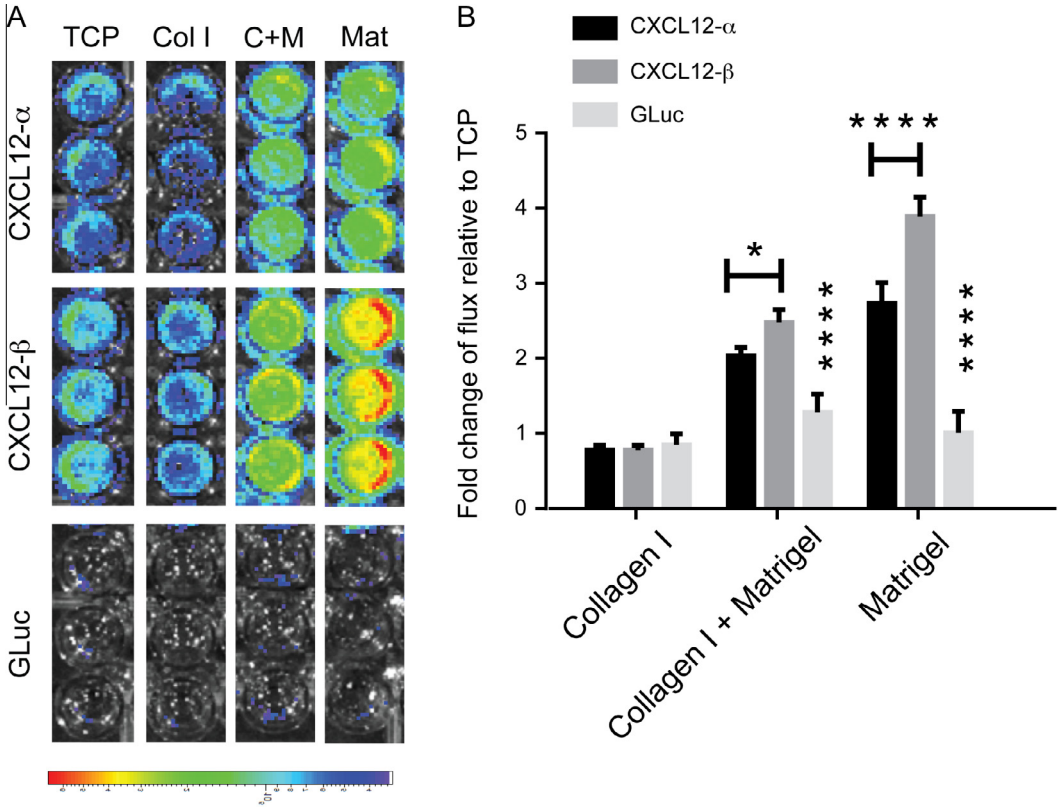

Fig. 5. Binding assay of CXCL12 isoforms in different gel matrices. (A) Representative heat map of flux plotted on the same log. (B) Fold change of flux relative to tissue culture plastic (TCP) for CXCL12-α, CXCL12- β and GL treated with collagen, collagen–Matrigel, and Matrigel. Values are plotted from one of three representative experiments as mean ± SEM for quadruplicate wells. Statistical demarcations above a bar indicate pairwise comparison to all others in that group. The bar indicates individual pairwise differences ($^{*}P < 0.05$, $^{**}P < 0.01$ and $^{****}P < 0.0001$).

ignored in this migration assay. Hence, migrating cells are forced to interact with the hydrogel matrix.

3.2. Migration rates depend on matrix composition and CXCL12 production

We first confirmed that cells could migrate through the patterned matrix by monitoring radial movement of MBA-231 cells initially patterned in a single spot (Fig. S3A). Radial dispersion of cells can be attributed to both random movement and growth of 231 cells (~24 h doubling time). To confirm that soluble factors can be transported through the matrix, the cytoskeletal disruption compound Latrunculin A was added to the culture and significantly suppressed radial migration (Fig. S3A-C). Confocal images of GL cells in collagen gel matrix at day 3 indicates most of the cells settled down on the surface with a 15 μm thick cell layer in the presence of Latruncurin, whereas cells radially migrated through the gel matrix in the absence of Latruncurin (data not shown). We seeded 6×10^4 cells per hydrogel-droplet in theory and, based on confocal imaging, confirmed that >99% (>5.9×10^4) of the cells settled down on the surface at t = 0. We also observed the same trend for other cell types used in this paper; this indicates that the observed cell migration did not arise from the randomly distributed suspended cells in hydrogels. Thus we assume that most cells settled down on the surface at t = 0, whereas they start to migrate in 3-D over the course of time.

Next, to examine effects of cell–matrix and ligand–matrix interactions on cell migration in hydrogel matrices, we patterned encapsulated CXCR4 + migrating cells adjacent to cells that secrete its ligand, CXCL12-β, which we express as a fusion to GL. CXCL12-β cells were used because the cells secrete the most chemokine compared to other CXCL12-isoforms [18]. In control experiments, we replaced the CXCL12-β source cells with cells secreting GL unfused to a chemokine, which does not bind to CXCR4 or regulate signaling through this receptor. To assess migration in this system, we measured the gap spacing between the leading edge of the migrating and source cell populations after 24 h and report the measured gap closure as the migration distance (Fig. 3A and B). CXCL12-β drove more rapid migration than the GL control in the presence of Matrigel. Without Matrigel, the migration rate was non-significant for CXCL12-β as compared to the GL control. This suggests that gradient generation and/or sensing of CXCL12-β requires interactions between CXCL12 and Matrigel components (Fig. 3C).

3.3. Matrix binding generates steep CXCL12 gradients

We hypothesized that Matrigel provides binding sites for CXCL12 factors, which influence the formation of both soluble and bound gradients in the matrix. To evaluate the potential contribution of ligand–matrix interactions in shaping the gradient, we used computational models to simulate diffusion and diffusion with a matrix-binding component. In the diffusion model, unbound CXCL12-β rapidly diffuses through the gel matrix, and generates a negligible specific gradient to stimulate cell migration (Fig. 4A). In contrast, ligand–matrix binding generates a steep specific gradient of unbound CXCL12-β, albeit at lower concentrations (Fig. 4B). Bound gradients may have similar profiles, but cannot precede the soluble gradient as diffusion across surfaces is well established to be significantly less than diffusion through an aqueous medium. These simulation results strongly indicate that interactions between the ligand and matrix facilitates gradient shaping and pre-

Please cite this article in press as: Kojima T et al. Surface-templated hydrogel patterns prompt matrix-dependent migration of breast cancer cells towards chemokine-secreting cells. Acta Biomater (2014), http://dx.doi.org/10.1016/j.actbio.2014.11.033

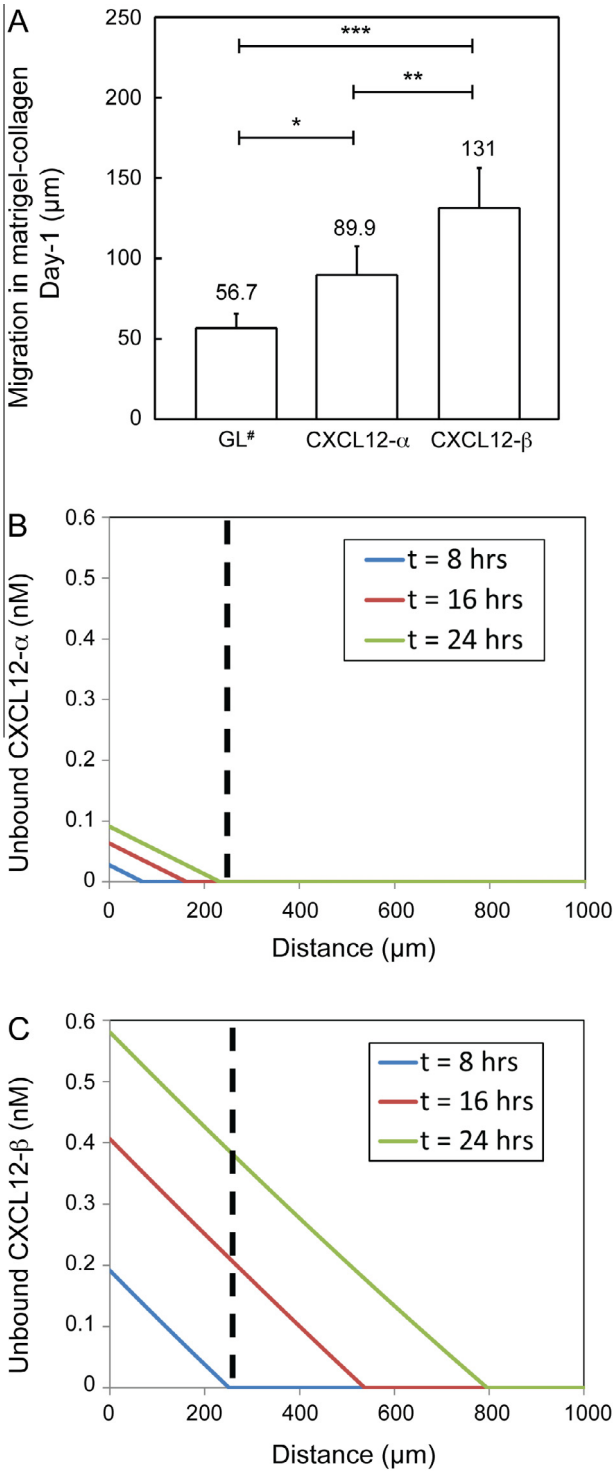

Fig. 6. Migratory comparison of CXCL12 isoforms in the presence of matrigel. (A) Migration assay of CXCR4-CXCL12 (GL, CXCL12-α and CXCL12-β) at day 1 in the presence of matrigel with 250 μm spacing ($^{*}P < 0.05$, $^{**}P < 0.01$ and $^{***}P < 0.001$). GL$^{\#}$ represents the replication of the data in Fig. 3C (+ matrigel/–CXCL12-β). (B-C) Computational simulation of unbound CXCL12-β and CXCL12-α gradient formation as a function of distance and time. Dotted line represents the spacing using between the patterned gels.

sents a possible mechanism explaining the matrix-dependent migratory differences observed in our chemotaxis experiments.

Additionally, our model suggests that when cell clusters are spaced >500 μm apart, chemotaxis cannot occur within the 24 h time-frame of the experiment, as steep gradients cannot form across large distances rapidly enough. To confirm the importance of this spacing, we doubled the spacing to 500 μm, and observed no significant migratory differences prompted by GL-secreting cells and CXCL12-expressing cells in 24 h (Fig. S4). Hence, the ability of our technique to position the cell clusters close to each other is a crucial parameter in observing these gradient-driven migratory responses.

3.4. Differential binding of CXCL12 isoforms to matrix components

To better understand the ligand–matrix interactions, we assessed the relative binding of CXCL12-isoforms to various matrix components. We used GL activity to measure the relative binding of secreted GL or CXCL12-s and CXCL12-β fused to GL to wells coated with collagen I alone, collagen I–Matrigel mixture and Matrigel alone (Fig. 5A). Note that this measurement was conducted on the hydrogel-coated 2-D well surface in contrast to other measurements in the 3-D hydrogel system. Collagen by itself provided no differential binding across all secreted factors (Fig. 5B). However, addition of Matrigel to collagen I caused a rank-order increase in binding, in which GL < CXCL12-α < CXCL12-β. Differential binding was statistically higher with Matrigel by itself as compared to collagen only and the collagen–Matrigel mixture. These findings suggest that Matrigel increases the capacity for CXCL12 binding and indicate that ligand–matrix interactions can be a dominant factor in shaping chemotactic gradients of CXCL12 isoforms. Furthermore, this suggests that matrix binding may provide a mechanism by which migration of CXCR4 cells in response to different CXCL12-isoforms may be altered.

3.5. Gradients of CXCL12 isoforms affect migration rate

To further explore the hypothesis that matrix-binding effects generate migration-inducing gradients, we compared the migration behavior in response to GL, CXCL12-α and CXCL12- β in the presence of Matrigel (Fig. 6A). We observed significant differences in migration associated with these secreted factors, in which the migration rate order is GL < CXCL12-α < CXCL12-β. These results are consistent with the results from the binding assay of these molecules to Matrigel presented in Sections 2.8 and 3.4. Simulations of gradient formation in the diffusive matrix-binding model revealed distinct gradient dynamics for CXCL12 isoforms, based on the secretion rate and binding kinetics of the isoforms (Fig. S5). These simulations indicate that CXCR4-β gradients from the source are established more rapidly than CXCR4-α gradients (Fig. 6B and C). Hence, in a relatively short-term experiment, migratory cells are exposed to chemotaxis-inducing gradients for different time periods, which likely explains the differences in migration observed between the α and β isoforms. While there may also be other effects of adding Matrigel, such as altered gel morphology or additional macromolecular crowding effects, taken together, our findings strongly suggest that our model system is able to adequately explore the parameters involved in matrix-sequestering gradient generation effects.

4. Discussion

We developed a novel patterning technique that exploits surface heterogeneity and cell-repellent properties to precisely pattern hydrogels for studies of gradient formation and cell migration. This system presents two core advantages over existing technologies for patterning cells: (i) broad applicability to a variety of ECM compositions and cell types; and (ii) facile patterning of multiple cell types in defined geometric locations. We exploit our ability to pattern cell-laden hydrogels of varying composition to

Please cite this article in press as: Kojima T et al. Surface-templated hydrogel patterns prompt matrix-dependent migration of breast cancer cells towards chemokine-secreting cells. Acta Biomater (2014), http://dx.doi.org/10.1016/j.actbio.2014.11.033

determine that formation of gradients of CXCL12 isoforms critically depends on ECM molecules for migration of CXCR4 + cells.

Our technology for patterning hydrogels relies on a simple surface patterning technology that biases cells and ligands towards interactions with the hydrogel matrix rather than the rigid substrate. By controlling relative surface energies between oxidized and native PAA-functionalized PDMS, we create geometrically defined hydrogel patterns while minimizing cell interactions with the solid substrate. This patterning technique is simpler than channel-based or laser lithography-based hydrogel patterning systems and provides more robust patterns than liquid–liquid patterning techniques, such as aqueous two-phase systems [32,38]. Simple but robust hydrogel patterning with our system decreases the barrier for adoption of 3-D assays and improves their flexibility for researchers. Moreover, given the biased interaction among patterned cells, their secreted factors and the hydrogel ECM, our system facilitates studies of the role of matrix interactions in physiological settings.

Dysregulated composition and architecture of the ECM is a fundamental hallmark of cancer. Perturbations in the ECM increase stiffness of the environment facilitate invasion of cancer cells along collagen fibrils and enhance tumor growth [39]. Less recognized is that changes in ECM content in tumors augment the capacity of the microenvironment to sequester growth factors in a way that increases local concentrations and establishes chemotactic gradients in pancreatic [40] and breast cancers [41,42]. For example, heparan sulfate proteoglycans in tumors binds CXCL12 and other soluble chemokines to create a chemotactic gradient that directs cell migration [43,44]. Our device enables facile control of ECM environments to study how interactions between chemotactic molecules and ECM molecules regulate the magnitude of chemokine gradients and resultant cell migration.

As a prime example of the interplay among migrating cells, cells secreting chemokines, and different ECM, we investigated migration of CXCR4 + cells towards gradients of different CXCL12-isoforms. We modulated the interaction between the CXCL12 and the ECM by incorporating Matrigel and expressing CXCL12 isoforms with different affinities for Matrigel. CXCL12-β, which has a higher affinity for matrigel than the α-isoform (Fig. 5), drove substantially higher migration of CXCR4 + cells. Our 3-D hydrogel system revealed another nuance of the source-sink model where CXCL12 gradient formation and sensing does not require CXCL12 scavenging by receptor CXCR7 as previously reported [4,5,18,45]. We found that for some CXCL12-isoforms, binding to the ECM may effectively form a gradient instead of CXCR7 ligand scavenging cells. Our system demonstrates how chemotactic phenotypes evolve differently among cell types in hydrogels and may better recreate in vivo physiology.

To further investigate effects of different ligand–matrix interactions on gradient dynamics, we developed a simple computational model of ligand diffusion away from cells secreting CXCL12 isoforms and binding to the ECM. Owing to the precisely patterned hydrogel matrix in 3-D and the large capacity for CXCL12 binding in the ECM, our computation and experimental model indicates that ligand–matrix interactions replace the cell-scavenging sink required in the previous 2-D assay. It should be noted that we cannot decouple the individual contribution of bound and free CXCL12 gradients, which is a limitation of this study. We assume that the combination of bound and unbound gradients of CXCL12 drive CXCR4 + migration (haptotaxis and chemotaxis, respectively). In the future work, bound gradients of CXCL12 can be generated in the hydrogel matrix to selectively assess CXCL12-dependent haptotaxis of CXCR4 + cells. This can be achieved through the use of 3-D ECM engineering techniques to tether gradients of molecules to the matrix [46–49].

Our system's flexibility extends to many different biological questions of how multicellular interactions in 3-D environments determine movement and morphogenesis, such as in angiogenesis [50,51], metastasis [52], and other processes [53] that require multiple patterns and cell populations. Here we use our system to analyze a tumor microenvironment to allow cell-autonomous gradient formation and sensing of chemotactic molecules. Our results support the idea that secreted signaling molecules interact with the ECM and direct cancer cell migration. We also note that our ECM patterning technique is amenable to multiplexing for studies of interactions between more than two cell-type or matrix combinations (Fig. S6).

5. Conclusions

Patterns on a non-adhesive surface can serve as a template to create patterns of cell-laden hydrogels with different gel compositions, cell types and soluble signals present. In this work, spatially patterned hydrogel matrices revealed distinct chemotactic behavior of breast cancer cells in response to production of the α- and β-isoforms of the soluble signaling factor CXCL12. Our computational models indicate that a steep gradient of CXCL12 forms as a result of ligand–matrix binding interactions in reconstituted ECM, and predicts a lag-time in gradient advancement between the CXCL12 isoforms. Our system establishes that autologous gradient formation arises as a result of this interaction, without the presence of cells that scavenge CXCL12. More broadly, our approach presents a simple alternative to generating microstructured biomaterials for advanced migratory and morphogenetic studies that can be easily adopted in a variety of wet-lab environments.

Acknowledgements

We thank the NIH for funding (CA136829 and CA170198). We gratefully acknowledge support from Yoshida Scholarship to T.K.; and from the Natural Sciences and Engineering Research Council, and Banting postdoctoral fellowship programs to C.M.; S.P.C. was supported on Advanced Proteome Informatics of Cancer Training Grant No. T32 CA140044 and an NSF Predoctoral Fellowship Project Grant No. F031543.

Appendix A. Figures with essential colour discrimination

Certain figure in this article, particularly Figs. 1–6 is difficult to interpret in black and white. The full colour images can be found in the on-line version, at http://dx.doi.org/10.1016/j.actbio.2014.11.033.

Appendix B. Supplementary data

Supplementary data associated with this article can be found, in the online version, at http://dx.doi.org/10.1016/j.actbio.2014.11.033.

References

[1] Kay RR, Langridge P, Traynor D, Hoeller O. Changing directions in the study of chemotaxis. Nat Rev Mol Cell Biol 2008;9:455–63.
[2] Weber M, Hauschild R, Schwarz J, Moussion C, de Vries I, Legler DF, et al. Interstitial dendritic cell guidance by haptotactic chemokine gradients. Science 2013;339:328–32.
[3] Fleury ME, Boardman KC, Swartz MA. Autologous morphogen gradients by subtle interstitial flow and matrix interactions. Biophys J 2006;91:113–21.
[4] Dona E, Barry JD, Valentin G, Quirin C, Khmelinskii A, Kunze A, et al. Directional tissue migration through a self-generated chemokine gradient. Nature 2013;503:285–9.

[5] Torisawa Y-s, Mosadegh B, Cavnar SP, Ho M, Takayama S. Transwells with microstamped membranes produce micropatterned two-dimensional and three-dimensional co-cultures. Tissue Eng Pt C-Meth 2010;17:61–7.
[6] Aubin H, Nichol JW, Hutson CB, Bae H, Sieminski AL, Cropek DM, et al. Directed 3D cell alignment and elongation in microengineered hydrogels. Biomaterials 2010;31:6941–51.
[7] Tang X, Ali MY, Saif MTA. A novel technique for micro-patterning proteins and cells on polyacrylamide gels. Soft matter 2012;8:7197–206.
[8] Nelson CM, VanDuijn MM, Inman JL, Fletcher DA, Bissell MJ. Tissue geometry determines sites of mammary branching morphogenesis in organotypic cultures. Science 2006;314:298–300.
[9] Lee GY, Kenny PA, Lee EH, Bissell MJ. Three-dimensional culture models of normal and malignant breast epithelial cells. Nat methods 2007;4:359–65.
[10] He J, Mao M, Liu Y, Shao J, Jin Z, Li D. Fabrication of nature-inspired microfluidic network for perfusable tissue constructs. Adv Healthc Mater 2013;2:1108–13.
[11] Zervantonakis IK, Hughes-Alford SK, Charest JL, Condeelis JS, Gertler FB, Kamm RD. Three-dimensional microfluidic model for tumor cell intravasation and endothelial barrier function. Proc Natl Acad Sci USA 2012;109:13515–20.
[12] Mosadegh B, Huang C, Park JW, Shin HS, Chung BG, Hwang S-K, et al. Generation of stable complex gradients across two-dimensional surfaces and three-dimensional gels. Langmuir 2007;23:10910–2.
[13] Saadi W, Rhee SW, Lin F, Vahidi B, Chung BG, Jeon NL. Generation of stable concentration gradients in 2D and 3D environments using a microfluidic ladder chamber. Biomed Microdevices 2007;9:627–35.
[14] Wang S-J, Saadi W, Lin F, Minh-Canh Nguyen C, Li Jeon N. Differential effects of EGF gradient profiles on MDA-MB-231 breast cancer cell chemotaxis. Exp Cell Res 2004;300:180–9.
[15] Barkefors I, Le Jan S, Jakobsson L, Hejll E, Carlson G, Johansson H, et al. Endothelial cell migration in stable gradients of vascular endothelial growth factor a and fibroblast growth factor 2 effects on chemotaxis and chemokinesis. J Biol Chem 2008;283:13905–12.
[16] Mosadegh B, Saadi W, Wang SÄ, Jeon NL. Epidermal growth factor promotes breast cancer cell chemotaxis in CXCL12 gradients. Biotechnol Bioeng 2008;100:1205–13.
[17] Torisawa Y-s, Mosadegh B, Bersano-Begey T, Steele JM, Luker KE, Luker GD, et al. Microfluidic platform for chemotaxis in gradients formed by CXCL12 source-sink cells. Integr Biol 2010;2:680–6.
[18] Cavnar S, Ray P, Moudgil P, Chang S, Luker K, Linderman J, et al. Microfluidic source-sink model reveals effects of biophysically distinct CXCL12 isoforms in breast cancer chemotaxis. Integr Biol 2014;6:564–76.
[19] Wylie RG, Ahsan S, Aizawa Y, Maxwell KL, Morshead CM, Shoichet MS. Spatially controlled simultaneous patterning of multiple growth factors in three-dimensional hydrogels. Nat Mater 2011;10:799–806.
[20] Hoffmann JC, West JL. Three-dimensional photolithographic micropatterning: a novel tool to probe the complexities of cell migration. Integr Biol 2013;5:817–27.
[21] Mosiewicz KA, Kolb L, van der Vlies AJ, Martino MM, Lienemann PS, Hubbell JA, et al. In situ cell manipulation through enzymatic hydrogel photopatterning. Nat Mater 2013;12:1072–8.
[22] Odawara A, Gotoh M, Suzuki I. Control of neural network patterning using collagen gel photothermal etching. Lab Chip 2013;13:2040–6.
[23] Pregibon DC, Toner M, Doyle PS. Magnetically and biologically active bead-patterned hydrogels. Langmuir 2006;22:5122–8.
[24] Akselrod G, Timp W, Mirsaidov U, Zhao Q, Li C, Timp R, et al. Laser-guided assembly of heterotypic three-dimensional living cell microarrays. Biophys J 2006;91:3465–73.
[25] Mirsaidov U, Scrimgeour J, Timp W, Beck K, Mir M, Matsudaira P, et al. Live cell lithography: using optical tweezers to create synthetic tissue. Lab Chip 2008;8:2174–81.
[26] Eng G, Lee BW, Parsa H, Chin CD, Schneider J, Linkov G, et al. Assembly of complex cell microenvironments using geometrically docked hydrogel shapes. Proc Natl Acad Sci USA 2013;110:4551–6.
[27] Khademhosseini A, Langer R. Microengineered hydrogels for tissue engineering. Biomaterials 2007;28:5087–92.
[28] Bong KW, Bong KT, Pregibon DC, Doyle PS. Hydrodynamic focusing lithography. Angew Chem 2010;122:91–4.
[29] Song JW, Cavnar SP, Walker AC, Luker KE, Gupta M, Tung Y-C, et al. Microfluidic endothelium for studying the intravascular adhesion of metastatic breast cancer cells. PLoS ONE 2009;4:e5756.
[30] Fiddes LK, Chan HKC, Lau B, Kumacheva E, Wheeler AR. Durable, region-specific protein patterning in microfluidic channels. Biomaterials 2010;31:315–20.
[31] Simmons CS, Ribeiro AJ, Pruitt BL. Formation of composite polyacrylamide and silicone substrates for independent control of stiffness and strain. Lab Chip 2013;13:646–9.
[32] Kojima T, Takayama S. Patchy surfaces stabilize dextran-polyethylene glycol aqueous two-phase system liquid patterns. Langmuir 2013;29:5508–14.
[33] Folch A, Toner M. Cellular micropatterns on biocompatible materials. Biotechnol Progr 1998;14:388–92.
[34] Raghavan S, Shen CJ, Desai RA, Sniadecki NJ, Nelson CM, Chen CS. Decoupling diffusional from dimensional control of signaling in 3D culture reveals a role for myosin in tubulogenesis. J Cell Sci 2010;123:2877–83.
[35] Laguri C, Sadir R, Rueda P, Baleux F, Renzana-Seisdedos Gans P, et al. The novel CXCL12gamma isoform encodes an unstructured cationic domain which regulates bioactivity and interaction with both glycosaminoglycans and CXCR4. PLoS ONE 2007;2:e1110.
[36] Adamson AW, Gast AP. Physical Chemistry of Surfaces. 6th edn. New York: John Wiley; 1997.
[37] Chiang EN, Dong R, Ober CK, Baird BA. Cellular responses to patterned poly (acrylic acid) brushes. Langmuir 2011;27:7016–23.
[38] Tavana H, Jovic A, Mosadegh B, Lee Q, Liu X, Luker K, et al. Nanoliter liquid patterning in aqueous environments for spatially-defined reagent delivery to mammalian cells. Nat Mater 2009;8:736–41.
[39] Lu P, Weaver VM, Werb Z. The extracellular matrix: a dynamic niche in cancer progression. J Cell Biol 2012;196:395–406.
[40] Koninger J, Giese T, di Mola FF, Wente MN, Esposito I, Bachem MG, et al. Pancreatic tumor cells influence the composition of the extracellular matrix. Biochem Biophys Res Commun 2004;322:943–9.
[41] Sasisekharan R, Shriver Z, Venkataraman G, Narayanasami U. Roles of heparan-sulphate glycosaminoglycans in cancer. Nat Rev Cancer 2002;2:521–8.
[42] Okolicsanyi RK, van Wijnen AJ, Cool SM, Stein GS, Griffiths LR, Haupt LM. Heparan sulfate proteoglycans and human breast cancer epithelial cell tumorigenicity. J Cell Biochem 2013;115:967–76.
[43] Kreuger J, Salmivirta M, Sturiale L, Gimenez-Gallego G, Lindahl U. Sequence analysis of heparan sulfate epitopes with graded affinities for fibroblast growth factors 1 and 2. J Biol Chem 2001;276:30744–52.
[44] Sadir R, Imberty A, Baleux F, Lortat-Jacob H. Heparan sulfate/heparin oligosaccharides protect stromal cell-derived factor-1 (SDF-1)/CXCL12 against proteolysis induced by CD26/dipeptidyl peptidase IV. J Biol Chem 2004;279:43854–60.
[45] Dambly-Chaudiere C, Cubedo N, Ghysen A. Control of cell migration in the development of the posterior lateral line: antagonistic interactions between the chemokine receptors CXCR4 and CXCR7/RDC1. BMC Dev Biol 2007;7:23.
[46] Luhmann T, Hall H. Cell guidance by 3D-gradients in hydrogel matrices: importance for biomedical applications. Materials 2009;2:1058–83.
[47] Luhmann T, Hanseler P, Grant B, Hall H. The induction of cell alignment by covalently immobilized gradients of the 6th Ig-like domain of cell adhesion molecule L1 in 3D-fibrin matrices. Biomaterials 2009;30:4503–12.
[48] DeLong SA, Moon JJ, West JL. Covalently immobilized gradients of bFGF on hydrogel scaffolds for directed cell migration. Biomaterials 2005;26:3227–34.
[49] Seidi A, Ramalingam M, Elloumi-Hannachi I, Ostrovidov S, Khademhosseini A. Gradient biomaterials for soft-to-hard interface tissue engineering. Acta Biomater 2011;7:1441–51.
[50] Raghavan S, Nelson CM, Baranski JD, Lim E, Chen CS. Geometrically controlled endothelial tubulogenesis in micropatterned gels. Tissue Eng Part A 2010;16:2255–63.
[51] Staton CA, Reed MW, Brown NJ. A critical analysis of current in vitro and in vivo angiogenesis assays. Int J Exp Pathol 2009;90:195–221.
[52] Sung S-Y, Hsieh C-L, Wu D, Chung LW, Johnstone PA. Tumor microenvironment promotes cancer progression, metastasis, and therapeutic resistance. Curr Prob Cancer 2007;31:36–100.
[53] Bhowmick NA, Neilson EG, Moses HL. Stromal fibroblasts in cancer initiation and progression. Nature 2004;432:332–7.

Please cite this article in press as: Kojima T et al. Surface-templated hydrogel patterns prompt matrix-dependent migration of breast cancer cells towards chemokine-secreting cells. Acta Biomater (2014), http://dx.doi.org/10.1016/j.actbio.2014.11.033